Epigenomic profiling of myelofibrosis reveals widespread DNA methylation changes in enhancer elements and *ZFP36L1* as a potential tumor suppressor gene epigenetically regulated

Nicolás Martínez-Calle[1,2#], Marien Pascual[1,2#], Raquel Ordoñez[1,2#], Edurne San José-Enériz[1,2], Marta Kulis[3], Estíbaliz Miranda[1,2], Elisabeth Guruceaga[4], Víctor Segura[4], María José Larráyoz[5], Beatriz Bellosillo[6], María José Calasanz[2,5], Carles Besses[7], José Rifón[2,8], José I. Martín-Subero[2,9,10], Xabier Agirre[1,2]*, Felipe Prosper[1,2,8]*.

[1]Área de Hemato-Oncología, Centro de Investigación Médica Aplicada, IDISNA, Universidad de Navarra, Avenida Pío XII-55, Pamplona, Spain.

[2]Centro de Investigación Biomédica en Red de Cáncer (CIBERONC).

[3]Fundació Clínic per a la Recerca Biomèdica, Barcelona, Spain

[4]Unidad de Bioinformática, Centro de Investigación Médica Aplicada, Universidad de Navarra, Avenida Pío XII-55, Pamplona, Spain.

[5]CIMA Lab Diagnostics, Universidad de Navarra, Pamplona, Spain.

[6]Departmento de Patología, Hospital del Mar, Barcelona, Spain.

[7]Departmento de Hematología, Hospital del Mar, Barcelona, Spain.

[8]Departamento de Hematología, Clínica Universidad de Navarra, Universidad de Navarra, Avenida Pío XII-36, Pamplona, Spain.

[9]Institut d'Investigacions Biomèdiques August Pi i Sunyer (IDIBAPS), Barcelona, Spain.

[10]Departament de Fonaments Clinics, Facultat de Medicina, Universitat de Barcelona, Barcelona, Spain.

# These authors share first authorship

* These authors share senior authorship

Running head

ZFP36L1 enhancer DNA methylation in MF.

Word Count:

- Manuscript: 3486
- Abstract: 193

Figure count: 3

Table count: 0

Supplementary figures: 1

Supplementary tables: 2

Reference count: 46

Correspondence and requests for materials should be addressed to:

X.A. (xaguirre@unav.es) or to F.P (fprosper@unav.es).

KEY POINTS:

- Epigenetic profiling of myelofibrosis patients reveals that aberrant DNA methylation is enriched in enhancer regions, outside traditional CpG islands.
- *ZFP36L1* is inactivated through DNA methylation of its enhancer region and represents a potential novel tumour suppressor, with a potential role in myelofibrosis.

ABSTRACT

In this study we have interrogated the DNA methylome of myelofibrosis patients using high-density DNA methylation arrays. We detected 35,215 differentially methylated CpGs corresponding to 10,253 genes between myelofibrosis patients and healthy controls. These changes were present both in primary and secondary myelofibrosis, which showed no differences between them. Remarkably, the majorities of differentially methylated CpGs were located outside gene promoter regions and showed a significant association with enhancer regions. This enhancer aberrant hypermethylation showed a negative correlation with the expression of 27 genes in the myelofibrosis cohort. Of these, we focused on *ZFP36L1* gene and validated its decreased expression and enhancer DNA hypermethylation in an independent cohort of patients and myeloid cell-lines. *In vitro* reporter assay and 5' azacitidine treatment confirmed the functional relevance of the enhancer hypermethylation of *ZFP36L1*. Furthermore, *in vitro* rescue of *ZFP36L1* expression had an impact in cell proliferation and induced apoptosis in SET-2 cell line indicating a possible role of *ZFP36L1* as a tumor suppressor gene in myelofibrosis. We describe the DNA methylation profile of myelofibrosis, identifying extensive changes in enhancer elements and revealing *ZFP36L1* as a novel candidate tumor suppressor gene.

INTRODUCTION

Philadelphia chromosome-negative myeloproliferative neoplasms (MPN), namely polycythemia vera (PV), essential thrombocythemia (ET) and primary myelofibrosis (MF) are characterized by a clonal transformation of hematopoietic progenitors leading to expansion of fully differentiated myeloid cells[1.] Primary MF carries the worst prognosis of all MPN, harboring progressive marrow fibrosis, extramedullary hematopoiesis, mild to severe splenomegaly and increased risk of leukemic transformation[2.] Secondary MF can also arise from PV and ET (post-PV or post-ET MF hereafter) by mechanisms that are still poorly understood and are clinically and morphologically indistinguishable from primary MF[3].

MF has been intensively studied from the genetic perspective[4,5], in fact, the modified WHO diagnostic criteria for MPN requires the demonstration of a genetic marker of clonal hematopoiesis (*JAK2V617F*, *CALR* or *MPL* mutations)[6]. The frequency of mutations on relevant epigenetic genes (i.e *DNMT3A*, *EZH2* and *ASXL1*), suggest that MF might have an epigenetic component that to our knowledge, remains poorly characterized[5]. Actually, epigenetic changes such as DNA methylation have been scarcely addressed in MF[7] partly due to the limited changes in promoter DNA methylation compared to other hematological malignancies, as previously published by our group[8]. DNA methylation of CpG islands (mostly on putative promoter regions) has been traditionally studied in both normal and neoplastic hematopoiesis[9,10]. However, high throughput platforms offer a wider coverage of the genome, allowing a better understanding of DNA methylation dynamics in regions distant from CpG islands[11]. In this regard, enhancer regions have been characterized as potentially relevant sites of DNA methylation outside CpG islands[12-14]. ChIP-seq studies have permitted the reliable mapping of genome-wide active enhancer regions based on histone modifications (i.e. H3K4me1 and H3K27Ac)[15,16], allowing the identification of enhancers playing a role in the dynamic transcriptional regulation during hematopoiesis[17].

The present work describes a comprehensive genome-wide analysis of DNA methylation

in MF patients, which has been coupled with gene expression analysis and information of functional chromatin states and compared with healthy donor samples[16]. Focusing on potential epigenetic alterations in enhancer regions, we identified *ZFP36L1* as potential tumor suppressor gene with relevance for the pathogenesis of MF.

METHODS

Patient samples and clinical data

MF patient samples (n=39) were composed of either bone marrow (BM), granulocytes or total peripheral blood (PB) cells. Among the MF cohort there were primary MF (n=22), MF post-ET (n=7) or MF post-PV (n=10). PB cells from healthy donors (n=6) were used as control samples in this study. All patients were diagnosed using the 2008 version of the World Health Organization (WHO) classification system of hematological malignancies[18]. Data for *JAK2V617F* mutation was retrospectively available for all patients, no data for CALR and MPL mutations was available. Patient's data are accessible from the Gene Expression Omnibus (GSE118241).

Samples and patient data were provided by the Biobank of the University of Navarra and were processed following standard operating procedures approved by the local Ethics & Scientific Committee. All patients consented prior to sample extraction and for the use of stored material for research purposes.

DNA Methylation profiling

DNA methylation was assessed with Human-Methylation 450K Bead-Chip kit (Illumina, Inc., San Diego, CA, USA) and the data was analyzed by Bioconductor open source software. The analytical pipeline implemented several filters to exclude technical and biological biases and taking into account the performance characteristics of Infinium I and Infinium II assays[19]. Differentially Methylated CpGs (DMC) were defined as previously described[13,19]. Details on the experimental procedures, annotation of CpG sites, detection of differentially methylated regions, and Gene Ontology analysis[20] are described in the online Supplementary Methods.

Identification of candidate genes targeted by aberrant DNA methylation in enhancers

Data of gene expression profiling from primary MF and healthy PB samples was obtained from the publicly available GEO accession bank number GSE26049[21]. Data was further processed using R and the open source Limma package[22]. Further details are described in online Supplementary Methods.

Luciferase reporter assays

The CpG-free vector (pCPG-L), gently provided by Dr. Michael Rehli[23], was used to clone the *ZFP36L1* enhancer region. Luciferase experiments were performed in triplicates and the details are described in the online Supplementary Methods. Primer sequences are available in **Supplementary Table 1**.

***ZFP36L1* binding motif search**

To further validate the potential relevance of *ZFP36L1* gene in MF, DREME motif-discovery algorithm[24] was used to assess enrichment of genes with the *ZFP36L1* consensus binding sequence among those genes differentially expressed in MF (FDR $\leq$ 0.05).

Overexpression of *ZFP36L1*

A vector containing *ZFP36L1* open reading frame was kindly provided by Dr. Murphy and sub-cloned into a PL-SIN-GK vector[25]. Further details are described in the online Supplementary Methods.

Statistical Analysis

For parametric group comparisons one-way ANOVA with Dunnet correction was used, whereas for non-parametric group comparisons Kruskall-Wallis test with Dunn correction was employed. Paired data was analyzed with Friedman non-parametric test with Dunn correction for multiple comparisons, for the data with single measurements. Two-way ANOVA with Tukey correction was used for data with multiple paired measurements. All tests were performed using Prism 7™ software (GraphPad, La Jolla, USA).

Details of other experimental procedures are given in the *Online Supplementary Methods.*

RESULTS AND DISCUSSION

MF is characterized by a specific DNA methylation pattern enriched in enhancer regions

In order to provide an exhaustive analysis of the DNA methylation profile in patients with MF, we analyzed the DNA methylome of patients with primary MF, secondary MF (including MF post-ET/post-PV) and healthy donors as controls, using the Human-Methylation 450K array. The first result worth highlighting is the epigenetic similarity, between primary and post-ET/post-PV myelofibrosis. Interestingly, with a FDR < 0.05, no differentially methylated CpGs (DMCs) between primary and secondary MF were found. Furthermore, we did not identify any CpG differentially methylated between post-ET and post-PV MF. However, both unsupervised principal component analysis (PCA) (**Figure 1A**) and hierarchical clustering study (**Supplementary Figure 1A**) using all CpGs analyzed confirmed an explicit segregation and a clear epigenetic difference between MF patient samples and healthy controls. These results allowed us hereafter to consider MF samples as a single sample cohort. Primary and secondary MFs are known to have very similar biological features, presenting symptoms and clinical course and in fact, both entities are treated indistinctively according to most published guidelines[26] . Nevertheless, some recent evidence from large retrospective trials has suggested that traditional prognostic factors may not be applicable to secondary MF as post-ET MF seems to have longer survival as compared to post-PV and primary MF[3,26-28]. Our current results are consistent with the similarities in the biological and clinical characteristics of primary and secondary MF, who are also remarkably homogenous in terms of their epigenetic profile, supporting a common biological origin[29].

Next, we sought to interrogate changes in DNA methylation between MF samples (considering primary and post-ET/PV MF as a single entity) and healthy controls**.** In this supervised analysis, we detected 35,215 DMCs (FDR $\leq$ 0.05) corresponding to 10,253 coding genes. Among all of these DMCs, 65.3% were hypomethylated (corresponding to 22,998 CpGs) and the remaining 34.7% were hypermethylated (a total of 12,217 CpGs), suggesting that loss of DNA methylation is the predominant alteration in this disease. Global DNA hypomethylation has also been a common finding in other hematological

malignancies such as chronic lymphocytic leukemia, multiple myeloma or acute myeloid leukemia[13,30,31].

Changes in DNA methylation levels are known to cooperate with the deposition of chromatin marks, particularly H3K4 methylation, to render the enhancers/promoters accessible/inaccessible for the transcription machinery[32-34]. Hence, the changes in DNA methylation observed in MF are very likely to impact the transcriptional profile of MF and potentially contribute to the malignant phenotype. In this context, differences in the DNA methylome between the novel MF subtypes defined by the new 2016 WHO classification (prefibrotic and over MF) remains to be characterized. This aspect exceeded the possibilities of our cohort, but warrants further investigation.

Even though previous studies have already interrogated the DNA methylation landscape of MF[35], their findings are limited to small numbers of epigenetic abnormalities mainly focused on the study of promoter regions. Our genome-wide approach of DNA methylation analysis using the 450k array allowed us to interrogate regulatory regions outside traditional promoters and obtain a deeper insight into the aberrant DNA methylome of MF. Therefore, in order to characterize the functionality of the detected DMCs, we performed a series of analyses. First, we analyzed their genomic location and identified that both hyper and hypomethylated CpGs were underrepresented in classical CGIs and significantly enriched outside CGIs (**Figure 1B**). This is an interesting finding, because traditionally, neoplasms acquire hypomethylation outside CGIs and hypermethylation in CGIs[13,31], and suggests that patterns of methylation gain in MF might differ to other neoplasms. To shed light into the specific function of the DMCs, chromatin state categorization of each CpG was done adapting a publicly available annotation of ChIP-seq data from CD34+ hematopoietic progenitor cells, in which four distinct states were defined: promoter (with H3K4me3), active enhancer (with H3K4me1 and H3K27ac), transcribed regions (showing H3K36me3) and heterochromatin (including H3K9me3 and H3K27me3)[16]. Both hyper and hypomethylated CpGs showed a significant enrichment in enhancer regions, together with a striking underrepresentation in promoter regions (**Figure 1B).** Unsupervised clustering of DMCs located exclusively

in enhancer regions **(Supplementary table 2)** displayed a clear segregation of the majority of MF patients from healthy controls (**Figure 1C**) identifying 4182 hyper and 10935 hypomethylated. This result reveals that patients with MF show an intrinsic aberrant pattern of DNA methylation preferentially located in enhancer regions of the genome.

To functionally characterize this aberrant DNA methylation of enhancer regions in MF, GO-PANTHER enrichment analysis was performed separately in differentially methylated genes. GO terms with an adjusted FDR < 0.05 were selected, showing in the case of hypermethylated enhancers interesting cellular processes such as cellular defense response or induction of apoptosis **(Figure 1D)**. Enhancer DNA methylation changes have been described to play a more prominent role in transcriptional regulation than promoter DNA methylation, governing processes such as hematopoietic differentiation and neoplastic transformation through the regulation of key transcription factors and genes[12,13,31,34,36]. These evidence translated into the context of MPN, might support the implication of aberrant enhancer DNA methylation in the abnormal pattern of differentiation leading to MF.

DNA methylation of enhancer regions is associated with gene expression profile in MF

Next, DNA methylation levels of enhancer regions were associated with the expression of host and adjacent coding genes using publicly available gene expression data of an independent cohort of MF patients and healthy donors (GSE26049)[21]. Fold increase in gene expression values were grouped according to the hypermethylated ($\Delta\beta > 0.4$) or hypomethylated ($\Delta\beta < -0.4$) enhancer status in MF versus controls. This analysis showed that enhancer DNA hypermethylation was associated with decreased gene expression of host/adjacent coding genes. In contrast, hypomethylated enhancer regions were not related to increased gene expression (**Figure 2A)**. These data suggest that aberrant DNA hypermethylation may be functionally more relevant than hypomethylation in MF. Enhancer hypermethylation has been reported in neutrophils[12], B-cells[37],AML cells[30] and myeloma[13] adding evidence to dynamic enhancer DNA hypermethylation as a relevant

regulatory mechanism of gene expression both in normal and neoplastic hematopoietic cells.

Next, we designed a more stringent approach to identify the set of genes underlying the most significant and substantial changes in enhancer DNA methylation (FDR < 0.01, $\Delta\beta$ > 0.4), coupled with downregulation of their expression (LogFC < 0) (**Figure 2B**). After identifying a number of potential candidates (27 genes), we focused on *ZFP36L1*, which codes for a RNA-binding protein that mediates the decay of unstable mRNAs with AU rich elements in the 3' untranslated region (3'UTR)[38,39]. *ZFP36L1* has been previously implicated in normal hematopoiesis[40] and specifically associated with erythroid and myeloid differentiation[41], suggesting a possible role of this gene in MF onset and progression. Moreover, *ZFP36L1* is also known to mediate mRNA decay of relevant genes for cell proliferation, survival and differentiation such as *CDK6*, *TNFα*, *BCL2*, *NOTCH1* and *STAT5B*[42,43]. Interestingly, the enhancer region associated with this candidate gene was located in its intragenic region, presumably acting as a *cis*-regulatory element of *ZFP36L1* transcription. Noteworthy, this regulatory element was consistently hypermethylated in the MF patient cohort and showed the largest number of hypermethylated enhancer-related CpG probes among the final 27-gene list. Such hypermethylation correlated with downregulation of *ZFP36L1* expression in MF as compared to controls (**Figure 2B and Supplementary Figure 1B**), which was further confirmed in an independent cohort of MF patients and myeloid cell lines (**Figure 2C**). Bisulfite sequencing confirmed that DNA methylation of the enhancer region of *ZFP36L1* was consistently higher in all MF samples and myeloid cell lines as compared to control samples, whereas the promoter region remained unmethylated (**Figure 2D-E, and Supplementary figure 1C**). Results obtained by luciferase-reporting assays demonstrated that the exogenous DNA methylation reduced significantly the *ZFP36L1* enhancer activity (**Figure 2F**). Moreover, 5´azacytidine hypomethylating treatment was able to reverse the DNA methylation levels of the enhancer region *in vitro*, restoring the gene expression levels of *ZFP36L1* in SET-2 cell line (**Figures 2G and 2H**). Although the potential implication of *ZFP36L1* in myeloid differentiation has been previously described[41], our results suggest that epigenetic downregulation of *ZFP36L1* might be a

prominent event in the pathobiology of MF; more importantly, hypermethylation of an enhancer regulatory element represents a novel mechanism for disruption of normal gene expression in the context of MF and *ZFP36L1*.

ZFP36L1 acts as a tumor suppressor gene in MPN

ZFP36L1 is known to mediate the degradation of mRNAs with AU rich elements in their 3'UTR. Therefore, we hypothesized that *ZFP36L1* downregulation could lead to upregulation of its putative targets in MF. To further validate this hypothesis, we used DREME, a motif discovery algorithm specifically designed to find short, core DNA-binding motifs enriched in the 3′UTR of genes. We found that the motif GTATTTDT (E-value = $4.5*10^{-15}$) was in fact overrepresented in transcripts upregulated in MF patients (**Figure 3A**). Subsequently, an analysis of motif enrichment was performed, revealing a significant enrichment of the mentioned motif ($p = 7.69*10^{-20}$) in transcripts upregulated in MF patients (log FC > 1; $p < 0.05$).

Moreover, as a complementary approach, we searched the database for AU-rich elements ARESite[44] to determine if, from the differentially expressed genes (B-value > 10) between MF and controls, we could detect an enrichment of these sequences in the upregulated subset of genes. Of all the possible AU motifs, we focused on the most restricted 9, 11 and 13-mer motifs. Interestingly, we were able to identify an enrichment of 9-mer sequence WTATTTATW ($p = 0.01$) and the 13-mer sequence WWWTATTTATWWW ($p = 0.03$) exclusively among the upregulated genes in MF patients (**Figure 3A**). Remarkably, both AU motifs highly resemble the core binding motif for *ZFP36L1* predicted by DREME algorithm, enforcing the regulatory role of this gene in MF. These results may suggest that *ZFP36L1* downregulation is involved in MF pathogenesis through a global deregulation of its transcriptome.

To further characterize the impact of *ZFP36L1* downregulation in MF, we tried to revert this phenotype by ectopic overexpression of the gene using lentiviral infection in the cell line SET-2. 72 hours post-infection, the levels of EGFP positive cells were evaluated to infer the efficacy of infection, together with the expression and protein levels of

ZFP36L1 to ensure the correct overexpression of the gene **(Figures 3B-D)**. Cell viability was measured for five consecutive days by MTS assay and a decrease of more than 50% in cell proliferation was observed, with an increase of AnnexinV positive cells as measured by flow cell cytometry (**Figures 3E and 3F**). Taken together, these results suggest that *ZFP36L1* downregulation can lead to significant alterations in the transcriptome, including relevant genes for cell proliferation, survival and differentiation, as previously described[41,42,45,46]. Consequently, when *ZFP36L1* expression levels are restored, SET-2 cells loss their malignant proliferative phenotype, enforcing the tumor suppressor role of this gene in MF.

CONCLUSION

The DNA methylation landscape of primary MF and post-ET/post-PV MF compared to healthy individuals show a consistent and differential DNA methylation profile between them. Absence of differences between primary MF and post-ET/post-PV MF suggests that these changes are founding epigenetic alterations occurring at the level of MPN stem cells and maintained in differentiated myeloid cells. Aberrant DNA methylation in MF is predominantly located in enhancer regions and has a significant impact on the expression of their target genes. Combining DNA methylation and gene expression data, we have identified *ZFP36L1* as an attractive new possible therapeutic target that shows a decrease of gene expression mediated by enhancer hypermethylation. Our results also suggest a direct effect of *ZFP36L1* downregulation in the gene expression profile of MF, through upregulation of mRNAs harbouring ARE canonical sites. For instance, *in vitro* rescue of *ZFP36L1* expression had an impact in cell proliferation and induced apoptosis in SET-2 cell line, indicating a possible role of *ZFP36L1* as a tumour suppressor gene in MF. Moreover, treatment with 5´azacytidine further evidenced the plausibility of *ZFP36L1* pharmacologic manipulation. Taken together, these results constitute an unexplored therapeutic target for MF patients, which remain to be properly evaluated in the pre-clinical scenario.

Acknowledgments

We particularly acknowledge the patients for their participation and the Biobank of the University of Navarra for its collaboration. We thank John J Murphy and Amor Alcaraz for providing *ZFP36L1* expression constructs. This research was funded by grants from Instituto de Salud Carlos III (ISCIII) PI14/01867, PI16/02024 and PI17/00701, TRASCAN (EPICA), CIBERONC (CB16/12/00489; Co-finance with FEDER funds), RTICC (RD12/0036/0068) and Departamento de Salud del Gobierno de Navarra 40/2016. N.M. is supported by a FEHH-Celgene research grant, M.P. was supported by a Sara Borrell fellowship CD12/00540 and RO was supported by Ministerio de Ciencia, Innovación y Universidades of Spain, Subprograma de Formación de Profesorado Universitario (FPU) award number FPU14/04331.

Authorship and Conflicts of Interest

The authors declare no competing conflicts of interests over the present manuscript.

REFERENCES

1 Spivak JL. Myeloproliferative Neoplasms. N Engl J Med. 2017;376(22):2168–2181.

2 Kim J, Haddad RY, Atallah E. Myeloproliferative neoplasms. Dis Mon. 2012;58(4):177–194.

3 Passamonti F, Rumi E, Caramella M, et al. A dynamic prognostic model to predict survival in post-polycythemia vera myelofibrosis. Blood. 2008;111(7):3383–3387.

4 Kim SY, Im K, Park SN, Kwon J, Kim J-A, Lee DS. CALR, JAK2, and MPL mutation profiles in patients with four different subtypes of myeloproliferative neoplasms: primary myelofibrosis, essential thrombocythemia, polycythemia vera, and myeloproliferative neoplasm, unclassifiable. Am J Clin Pathol. 2015;143(5):635–644.

5 Vainchenker W, Kralovics R. Genetic basis and molecular pathophysiology of classical myeloproliferative neoplasms. Blood. 2017;129(6):667–679.

6 Arber DA, Orazi A, Hasserjian R, et al. The 2016 revision to the World Health Organization classification of myeloid neoplasms and acute leukemia. Blood. 2016;127(20):2391–2405.

7 Myrtue Nielsen H, Lykkegaard Andersen C, Westman M, et al. Epigenetic changes in myelofibrosis: Distinct methylation changes in the myeloid compartments and in cases with ASXL1 mutations. Sci Rep. 2017;7(1):6774.

8 Pérez C, Pascual M, Martín-Subero JI, et al. Aberrant DNA methylation profile of chronic and transformed classic Philadelphia-negative myeloproliferative neoplasms. Haematologica. 2013;98(9):1414–1420.

9 Mendizabal I, Yi SV. Whole-genome bisulfite sequencing maps from multiple human tissues reveal novel CpG islands associated with tissue-specific regulation. Hum Mol Genet. 2016;25(1):69–82.

10 Deaton AM, Webb S, Kerr ARW, et al. Cell type-specific DNA methylation at intragenic CpG islands in the immune system. Genome Res. 2011;21(7):1074–1086.

11 Sandoval J, Heyn H, Moran S, et al. Validation of a DNA methylation microarray for 450,000 CpG sites in the human genome. Epigenetics. 2011;6(6):692–702.

12 Rönnerblad M, Andersson R, Olofsson T, et al. Analysis of the DNA methylome and transcriptome in granulopoiesis reveals timed changes and dynamic enhancer methylation. Blood. 2014;123(17):e79–e89.

13 Agirre X, Castellano G, Pascual M, et al. Whole-epigenome analysis in multiple myeloma reveals DNA hypermethylation of B cell-specific enhancers. Genome Res. 2015;25(4):478–487.

14 Bell RE, Golan T, Sheinboim D, et al. Enhancer methylation dynamics contribute to cancer plasticity and patient mortality. Genome Res. 2016;26(5):601–611.

15 Ernst J, Kheradpour P, Mikkelsen TS, et al. Mapping and analysis of chromatin state dynamics in nine human cell types. Nature. 2011;473(7345):43–49.

16 Wijetunga NA, Delahaye F, Zhao YM, et al. The meta-epigenomic structure of purified human stem cell populations is defined at cis-regulatory sequences. Nat Commun. 2014;5:5195.

17 Lara-Astiaso D, Weiner A, Lorenzo-Vivas E, et al. Immunogenetics. Chromatin state dynamics during blood formation. Science. 2014; 345(6199):943–949.

18 Tefferi A, Thiele J, Vardiman JW. The 2008 World Health Organization classification system for myeloproliferative neoplasms. Cancer. 2009;115(17):3842–3847.

19 Kulis M, Merkel A, Heath S, et al. Whole-genome fingerprint of the DNA methylome during human B cell differentiation. Nat Genet. 2015;47(7):746–756.

20 Mi H, Huang X, Muruganujan A, et al. PANTHER version 11: expanded annotation data from Gene Ontology and Reactome pathways, and data analysis tool enhancements. Nucleic Acids Res. 2017;45(D1):D183–D189.

21 Skov V, Larsen TS, Thomassen M, et al. Whole-blood transcriptional profiling of interferon-inducible genes identifies highly upregulated IFI27 in primary myelofibrosis. Eur J Haematol. 2011;87(1):54–60.

22 Ritchie ME, Phipson B, Wu D, et al. limma powers differential expression analyses for RNA-sequencing and microarray studies. Nucleic Acids Res. 2015;43(7):e47.

23 Klug M, Rehli M. Functional analysis of promoter CpG methylation using a CpG-free luciferase reporter vector. Epigenetics. 2006;1(3):127–130.

24 Bailey TL. DREME: motif discovery in transcription factor ChIP-seq data. Bioinformatics. 2011;27(12):1653–1659.

25 Hotta A, Cheung AYL, Farra N, et al. Isolation of human iPS cells using EOS lentiviral vectors to select for pluripotency. Nat Methods. 2009;6(5):370–376.

26 Reilly JT, McMullin MF, Beer PA, et al. Use of JAK inhibitors in the management of myelofibrosis: a revision of the British Committee for Standards in Haematology Guidelines for Investigation and Management of Myelofibrosis 2012. Br J Haemat. 2014;167(3):418–420.

27 Hernández-Boluda J-C, Pereira A, Gómez M, et al. The International Prognostic Scoring System does not accurately discriminate different risk categories in patients with post-essential thrombocythemia and post-polycythemia vera myelofibrosis.

Haematologica. 2014;99(4):e55–e57.

28 Passamonti F, Giorgino T, Mora B, et al. A clinical-molecular prognostic model to predict survival in patients with post polycythemia vera and post essential thrombocythemia myelofibrosis. Leukemia. 2017;31(12):2726–2731.

29 Brecqueville M, Rey J, Devillier R, et al. Array comparative genomic hybridization and sequencing of 23 genes in 80 patients with myelofibrosis at chronic or acute phase. Haematologica. 2014;99(1):37–45.

30 Qu Y, Siggens L, Cordeddu L, et al. Cancer-specific changes in DNA methylation reveal aberrant silencing and activation of enhancers in leukemia. Blood. 2017;129(7):e13–e25.

31 Kulis M, Heath S, Bibikova M, et al. Epigenomic analysis detects widespread gene-body DNA hypomethylation in chronic lymphocytic leukemia. Nat Genet. 2012;44(11):1236–1242.

32 Sharifi-Zarchi A, Gerovska D, Adachi K, et al. DNA methylation regulates discrimination of enhancers from promoters through a H3K4me1-H3K4me3 seesaw mechanism. BMC Genom. 2017;18(1):964.

33 King AD, Huang K, Rubbi L, et al. Reversible Regulation of Promoter and Enhancer Histone Landscape by DNA Methylation in Mouse Embryonic Stem Cells. Cell Rep. 2016;17(1):289–302.

34 Blattler A, Yao L, Witt H, et al. Global loss of DNA methylation uncovers intronic enhancers in genes showing expression changes. Genome Biol. 2014;15(9):469.

35 Myrtue Nielsen H, Lykkegaard Andersen C, Westman M, et al. Epigenetic changes in myelofibrosis: Distinct methylation changes in the myeloid compartments and in cases with ASXL1 mutations. Sci Rep. 2017;7(1):6774.

36 Hon GC, Rajagopal N, Shen Y, et al. Epigenetic memory at embryonic enhancers identified in DNA methylation maps from adult mouse tissues. Nat Genet. 2013;45(10):1198–1206.

37 Bergmann AK, Castellano G, Alten J, et al. DNA methylation profiling of pediatric B-cell lymphoblastic leukemia with KMT2A rearrangement identifies hypomethylation at enhancer sites. Pediatr Blood Cancer. 2017;64(3):e26251.

38 Hitti E, Bakheet T, Al-Souhibani N, et al. Systematic Analysis of AU-Rich Element Expression in Cancer Reveals Common Functional Clusters Regulated by Key RNA-Binding Proteins. Cancer Res. 2016;76(14):4068-4080.

39 Baou M, Norton JD, Murphy JJ. AU-rich RNA binding proteins in hematopoiesis and leukemogenesis. Blood. 2011;118(22):5732–5740.

40 Galloway A, Saveliev A, Łukasiak S, et al. RNA-binding proteins ZFP36L1 and ZFP36L2 promote cell quiescence. Science. 2016;352(6284):453–459.

41 Vignudelli T, Selmi T, Martello A, et al. ZFP36L1 negatively regulates erythroid differentiation of CD34+ hematopoietic stem cells by interfering with the Stat5b pathway. Mol Biol Cell. 2010;21(19):3340–3351.

42 Zekavati A, Nasir A, Alcaraz A, et al. Post-transcriptional regulation of BCL2 mRNA by the RNA-binding protein ZFP36L1 in malignant B cells. PLoS One. 2014;9(7):e102625.

43 Liu J, Lu W, Liu S, et al. ZFP36L2, a novel AML1 target gene, induces AML cells apoptosis and inhibits cell proliferation. Leuk Res. 2018;68:15–21.

44 Gruber AR, Fallmann J, Kratochvill F, Kovarik P, Hofacker IL. AREsite: a database for the comprehensive investigation of AU-rich elements. Nucleic Acids Res. 2011;39(Database issue):D66–D69.

45 Chen M-T, Dong L, Zhang X-H, et al. ZFP36L1 promotes monocyte/macrophage differentiation by repressing CDK6. Sci Rep. 2015;5(1):16229.

46 Hodson DJ, Janas ML, Galloway A, et al. Deletion of the RNA-binding proteins ZFP36L1 and ZFP36L2 leads to perturbed thymic development and T lymphoblastic leukemia. Nat Immunol. 2010;11(8):717–724.

LEGENDS TO THE FIGURES

Figure 1. MF harbors a differential DNA methylation profile compared to control samples, with changes located primarily on enhancer regions. A) Unsupervised principal component analysis (PCA) showing a differential DNA methylation profile of MF patients and healthy controls with no differences between primary and secondary MF. **B)** Distribution of DMCs according to CpG island mapping (left graph) or functional chromatin analysis (right graph) grouped by DNA methylation status of the probes (legend). *$p < 0.05$ **C)** Hierarchical clustering of DMC located to enhancer regions in MF patients and healthy controls. **D)** GO-PANTHER analysis of genes adjacent to enhancer-DMCs. Analysis of hypermethylated and hypomethylated genes is shown on the left and right panel respectively.

Figure 2. Aberrant enhancer DNA methylation regulates gene expression in MF. A) Violin density plots of expression of genes with differentially methylated CpGs located to enhancer regions. Vertical axis represents fold change in gene expression. The horizontal width of the plot represents density of data along the y axis. **B)** Candidate genes with substantial changes in DNA methylation (FDR < 0.01) and differential gene expression. Red bars represent average of DNA methylation of all enhancer-mapped probes and black bars the average expression of all probes, error bars represent SD. **C)** *ZFP36L1* downregulation validation by RT-qPCR in MF patients and 3 myeloid cell lines (including SET-2) compared to healthy controls (HC) (n=3). **D-E)** Bisulfite sequencing of *ZFP36L1* **D)** enhancer region and **E)** promoter region in healthy controls (HC), cell lines and primary MF samples. For each sample, graph shows mean ± SD of 10 CpG dinucleotides for enhancer region and 15 CpG dinucleotides for promoter region. **F)** pCpG-L luciferase reporter assay showing the inhibition of luciferase activity after treatment of *ZFP36L1* enhancer region with Sss-I methyltransferase. **G)** DNA methylation levels of the enhancer region (same 10 CpG dinucleotides as in **D)** after 5́azacytidine (AZA) treatment of SET-2. **H)** *ZFP36L1* expression levels after 5′azacytidine (AZA) treatment of SET-2. Plots/bars indicate mean ± SD.

Figure 3. *ZFP36L1* decreases cell viability in MF. A) Consensus binding motif for ZFP36L1 obtained by DREME motif discovery among transcripts with putative AU-rich motifs upregulated in MF samples. **B)** Efficiency of infection measured by percentage of EGFP positive cells after lentiviral infection. **C)** Q-PCR validation of *ZFP36L1* restoration in SET-2 cell line after lentiviral infection. **D)** ZFP36L1 protein restoration measured by Western Blot in SET-2 cell line after lentiviral infection. **E)** ZFP36L1 rescue in SET-2 cell line decreased cell proliferation rate and **F)** increased AnnexinV positive cells.

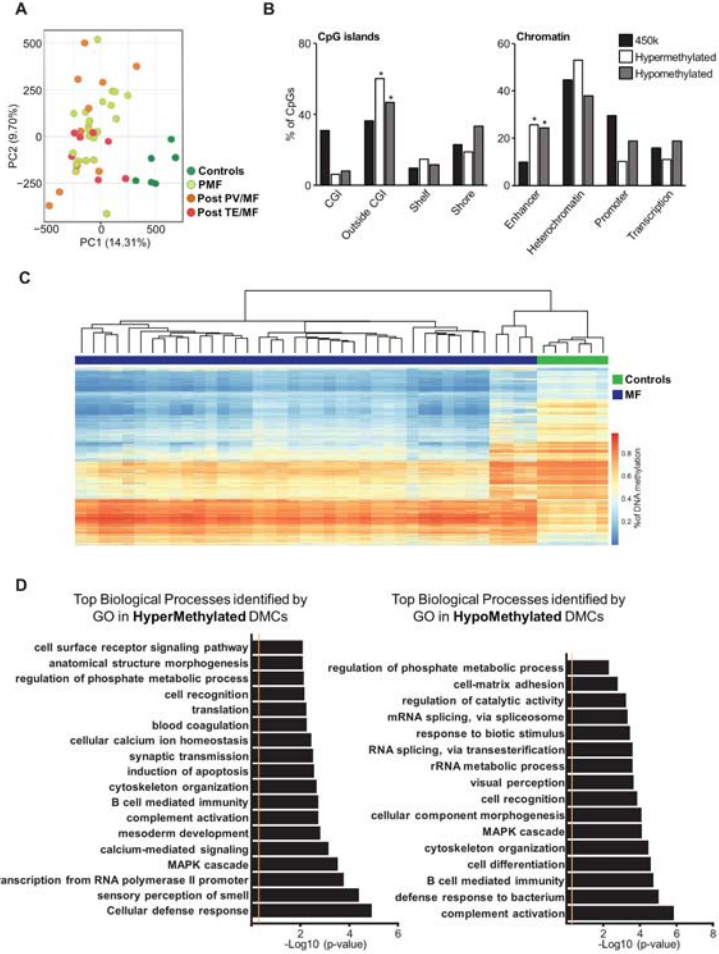
A
PC2 (9.70%)
PC1 (14.31%)
Controls
PMF
Post PV/MF
Post TE/MF
B
CpG islands
% of CpGs
CGI
Outside CGI
Shelf
Shore
Chromatin
450k
Hypermethylated
Hypomethylated
Enhancer
Heterochromatin
Promoter
Transcription
C
Controls
MF
%of DNA methylation
D
Top Biological Processes identified by GO in HyperMethylated DMCs
cell surface receptor signaling pathway
anatomical structure morphogenesis
regulation of phosphate metabolic process
cell recognition
translation
blood coagulation
cellular calcium ion homeostasis
synaptic transmission
induction of apoptosis
cytoskeleton organization
B cell mediated immunity
complement activation
mesoderm development
calcium-mediated signaling
MAPK cascade
transcription from RNA polymerase II promoter
sensory perception of smell
Cellular defense response
-Log10 (p-value)
Top Biological Processes identified by GO in HypoMethylated DMCs
regulation of phosphate metabolic process
cell-matrix adhesion
regulation of catalytic activity
mRNA splicing, via spliceosome
response to biotic stimulus
RNA splicing, via transesterification
rRNA metabolic process
visual perception
cell recognition
cellular component morphogenesis
MAPK cascade
cytoskeleton organization
cell differentiation
B cell mediated immunity
defense response to bacterium
complement activation
-Log10 (p-value)

FIGURE 1

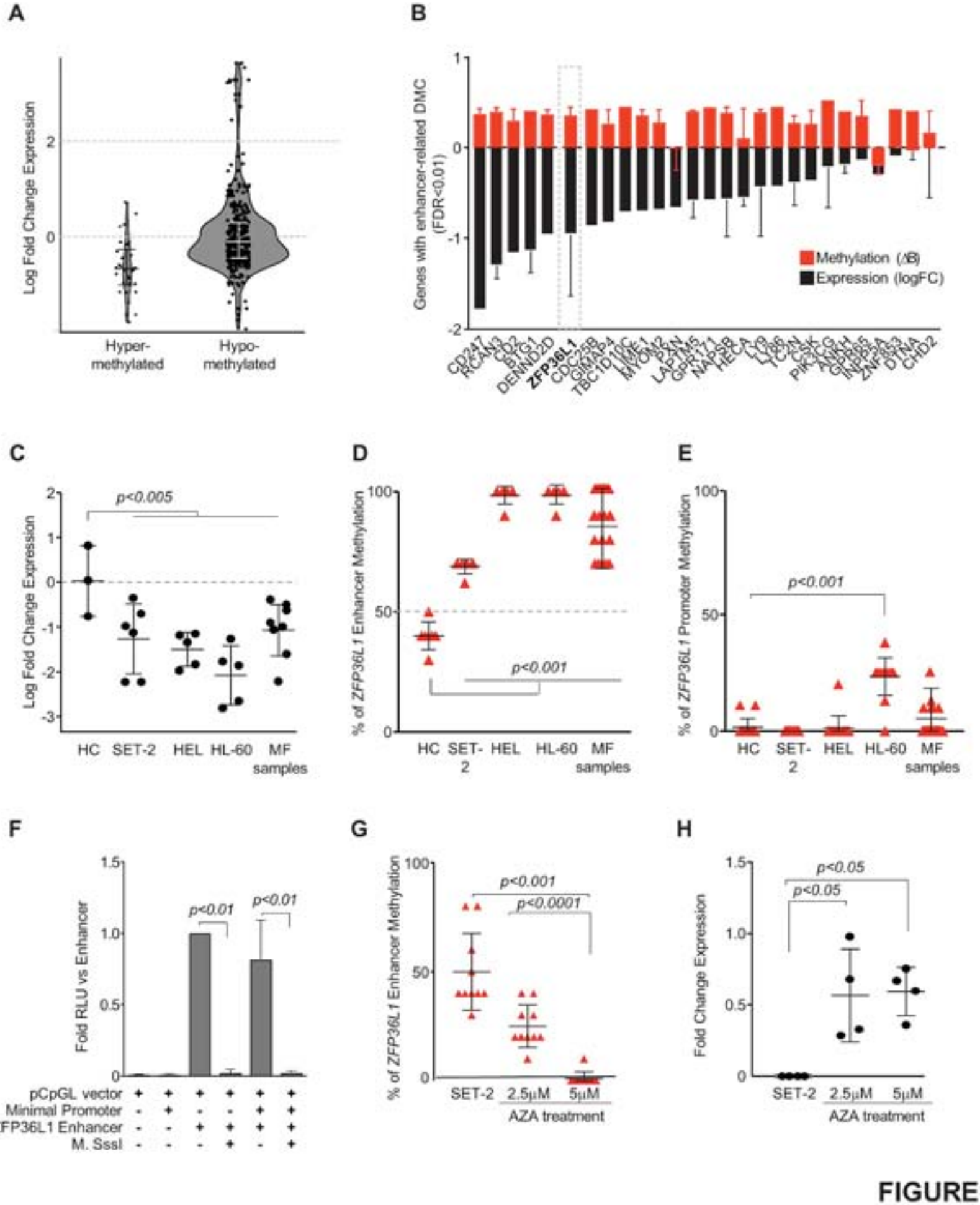
A
Log Fold Change Expression
2
0
Hyper-methylated
Hypo-methylated
B
Genes with enhancer-related DMC (FDR<0.01)
1
0
-1
-2
Methylation (Δβ)
Expression (logFC)
CD247
RCAN3
CD2
BTG1
DENND2D
ZFP36L1
CDC25B
GIMAP4
TBC1D10C
LIME1
MYO9B
PXN
LAPTM5
GPR171
NAP5B
HECA
LY9
LY86
TCF7
CSK
PIK3CG
ANKH
GPR65
INPP5A
ZNF853
DTNA
CHD2
C
Log Fold Change Expression
p<0.005
HC
SET-2
HEL
HL-60
MF samples
D
% of ZFP36L1 Enhancer Methylation
p<0.001
HC
SET-2
HEL
HL-60
MF samples
E
% of ZFP36L1 Promoter Methylation
p<0.001
HC
SET-2
HEL
HL-60
MF samples
F
Fold RLU vs Enhancer
p<0.01
p<0.01
pCpGL vector
Minimal Promoter
ZFP36L1 Enhancer
M. SssI
G
% of ZFP36L1 Enhancer Methylation
p<0.001
p<0.0001
SET-2
2.5μM
5μM
AZA treatment
H
Fold Change Expression
p<0.05
p<0.05
SET-2
2.5μM
5μM
AZA treatment

FIGURE 2

A

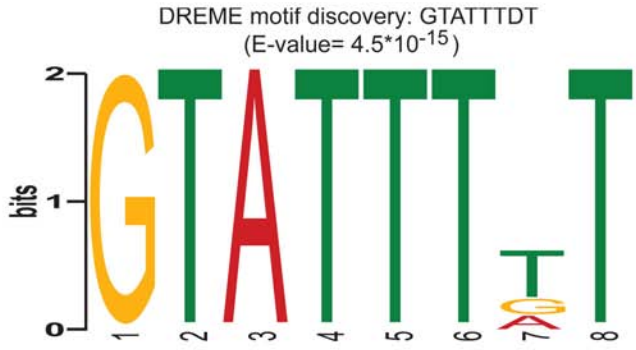

Motif	Targets in Selection	p-value
ATTTA	265	**1.03E-08**
WWATTTAWW	**139**	**0.04**
WTATTTATW	70	**0.010**
WWTATTTATWW	37	N.S
WWWTATTTATWWW	24	**0.039**

B

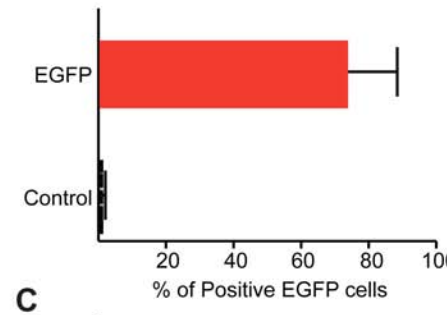

C

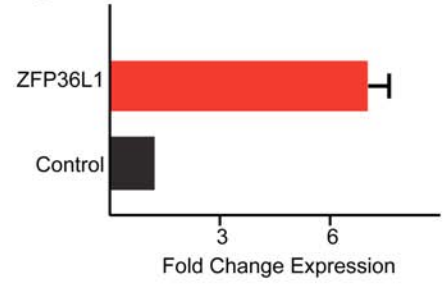

D

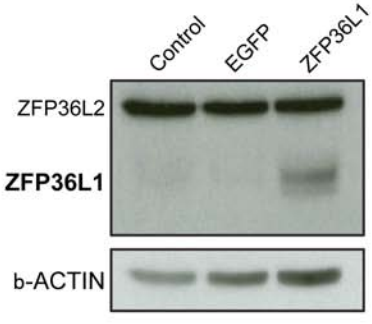

E

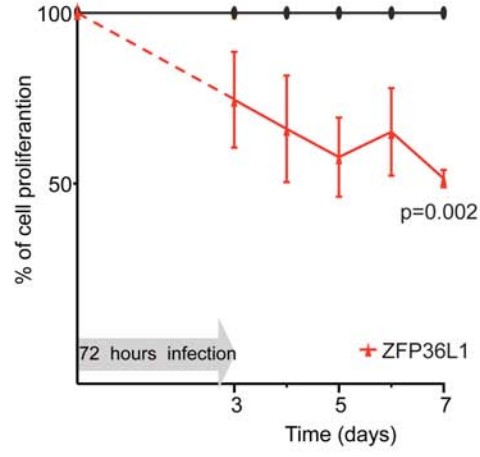

F

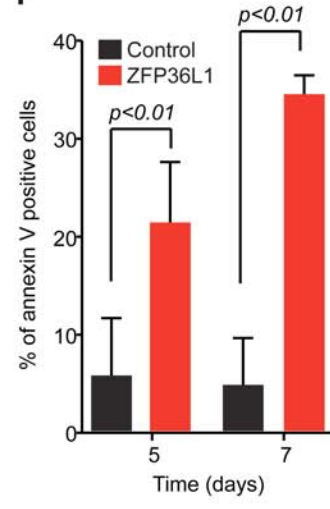

FIGURE 3

SUPPLEMENTARY METHODS

DNA Methylation profiling

DNA methylation was assessed with Human-Methylation 450K Bead-Chip kit (Illumina, Inc., San Diego, CA, USA). The array-based assays for DNA methylation profiling were performed at the National Centre of Oncologic Investigations (CNIO, Madrid, Spain). Briefly, 500ng of genomic DNA were modified with sodium bisulfite (EZ DNA Methylation Kit, Zymo Research) and subsequently whole genome amplified following manufacturer's recommendations. Samples were then hybridized in the assay chips as previously described[1]. Data arising from the 450K Human-Methylation array was analyzed by Bioconductor open source software. The analytical pipeline implemented several filters to exclude technical and biological biases (i.e. sex-specific methylation or overlapping CpGs with SNPs) and taking into account the performance characteristics of Infinium I and Infinium II assays[2]. Differentially Methylated CpGs (DMC) were defined as previously described[2,3]. DNA methylation data sets are available from the Gene Expression Omnibus (GSE118241).

Genomic and functional annotation of CpG sites

The hg19 version of the UCSC Genome Browser database was used to annotate raw data from the DNA methylation array. DMCs were annotated into four categories relative to CpG islands (CGI) as follows: inside CGI, CGI-shore (0-2 Kb from the CGI), CGI-shelf (>2 Kb up to 4 Kb from the CGI) and outside CGI (>4kb from the CGI). All annotations were extracted from Ensembl database (http://www.ensembl.org). DMCs were also annotated according to publicly available functional chromatin states of human CD34+ cells following the ChromHMM algorithm[4,5]. Chromatin states were categorized in six functional features (0: heterochromatin; 1-3: transcription-start sites; 4-5: enhancer regions (weak and strong); 6: promoters). This final annotation led to the identification of a group of DMC between MF and healthy controls that mapped to enhancer regions. The genes adjacent to these enhancers were then used for Gene Ontology (GO) functional enrichment analysis (GO-PANTHER) as described elsewhere[6].

Identification of candidate genes targeted by aberrant DNA methylation in enhancers

Data of gene expression profiling (Affymetrix gene expression array) from primary MF (n=9) and healthy peripheral blood samples (n=21) was obtained from the publicly available GEO accession bank number GSE26049[7]. Data was further processed using R and the open source Limma package[8]. Genes showing consistent and ample differences in DNA methylation between MF and the control group were included (FDR<0.01; $\Delta\beta$>0.4) and then were subsequently filtered by the changes in gene expression (logFC values below 0). The final list included 31 probes, encompassing 27 coding genes. Each of these genes was subsequently explored by literature search to identify those with potential implication in the hematopoietic system.

Cell culture

The SET-2 cell line (DMSZ # ACC-608; established from the peripheral blood of a patient diagnosed with essential thrombocythemia at megakaryoblastic leukemic transformation) was maintained in RPMI medium supplemented with 20% fetal bovine serum and antibiotics (100 IU/mL penicillin, 50 µg/mL streptomycin). HEL (DSMZ # ACC-11) and HL-60 (DSMZ # ACC-3) cell lines were maintained in RPMI medium supplemented with 10% fetal bovine serum and antibiotics (100 IU/mL penicillin, 50 µg/mL streptomycin). Cells were seeded at $0.5x10^6$ cells/ml and incubated at 37^oC and 5% CO_2 with 95% humidity.

Bisulfite sequencing

DNA methylation levels were interrogated and validated using traditional bisulfite sequencing. Briefly, after bisulfite modification (CpGenome DNA modification Kit, Merck, Darmstadt, Germany), the fragment of interest was amplified, sub-cloned into the pGEM-T easy vector system (Promega, Madison, USA) and transformed in JM109 competent cells (Promega, Madison, USA). Plasmid DNA was extracted (Nucleospin Plasmid, Macherey Nagel, Germany) and for each condition, at least 10 different CFUs (colony forming units) were sequenced by classical Sanger method using Genetic Analyzer 3130XL (Life Technologies, Carlsbad, USA). Universally methylated human DNA (Zymo research, USA) was used as a positive DNA methylation control for bisulfite modification. Primer sequences are available in **Supplementary Table 1**.

Luciferase reporter assays

The CpG-free vector (pCPG-L), gently provided by Dr. Michael Rehli[9], was used to clone the *ZFP36L1* enhancer region, after amplification with high-fidelity Platinum™ Taq polymerase (Invitrogen, Walthman, USA). Cloned plasmids were amplified on PIR1 competent *E. coli* cells (Invitrogen, Carlsbad, USA) and then treated with SssI CpG methyltransferase enzyme (New England Biolabs, Ipswich, USA) following manufacturer´s instructions. HEK293T cells were co-transfected with 10 ng/µl of DNA methylated or unmethylated reporter plasmids and 0.5 ng/µl renilla luciferase vector (pRL-SV40 Renilla Luciferase Control Reporter Vector, Promega), using Lipofectamine- 2000 (Invitrogen, Carlsbad, CA). Forty-eight hours after transfection, luciferase/Renilla activity was analyzed using the Dual Luciferase® reporter assay system (Promega, Madison, USA) in an automatic 96-well plate reader according to manufacturer's instructions. Luciferase experiments were performed in triplicates. Primer sequences are available in **Supplementary Table 1**.

Gene expression by Q-PCR

Quantitative PCRs (Q-PCR) were performed with SYBR Green Master Mix (Applied Biosystems, Foster City, USA) and QuantStudio-3 96-well real-time PCR system (Applied Biosystems, Foster City, USA). *GUSB* gene was used as housekeeping reference gene in all cases. Primer sequences are available in **Supplementary Table 1**.

Overexpression of *ZFP36L1*

A vector containing *ZFP36L1* open reading frame was kindly provided by Dr. Murphy and sub-cloned into a PL-SIN-GK vector[10]. The same vector backbone carrying an EGFP open reading frame was used as experimental control. Lentiviral particles were generated by co-transfecting HEK293T cells with ZFP36L1-encoding plasmid, psPAX2 (Addgene, #12260) and pMD2G (Addgene, #12259) plasmids (3:2:1 ratio) using Lipofectamine-2000 (Invitrogen, Carlsbad, CA). Viral supernatant was harvested after 72h, filtered (0.2 µm), concentrated by ultra-centrifugation (26,000 g for 2.5 hours at 4 ^{o}C) and supplemented to the cells for infection with polybrene (Sigma-Aldrich, Saint Louis, USA) at 4 µg/ml. SET-2 cell line was used as an *in vitro* model of *JAK2V617F* mutated MPN. Infection efficiency was assessed after 72h, determining EGFP positive

cells by FACScanto-II™ flow cytometer (BD Biosciences, San Jose, USA) and CellQuest software™ (Becton Dickinson, Franklin Lakes, USA).

Apoptosis and cell proliferation assays

Apoptosis was assessed using the FITC Annexin V Apoptosis Detection Kit I (BD Biosciences, San Jose, USA) following manufacturer´s protocol. Apoptosis was analyzed using FACScantoTM flow cytometer and CellQuest softwareTM (Becton Dickinson, Franklin Lakes, USA). Cellular proliferation was assessed with standard MTS assays using the CellTiter 96® AQueous MTS Reagent (Promega, Madison, USA). All experiments were performed in triplicates.

Western Blotting

After standard protein extraction, 50μg of protein were separated by 10% SDS-PAGE electrophoresis and transferred onto a nitrocellulose membrane (Bio-Rad, Hercules, USA). Membranes were incubated with the primary antibodies as follows: polyclonal rabbit anti ZFP36L1/ZFP36L2 (#2119 Cell Signaling, Leiden, Netherlands), loading control was made with mouse anti β-actin antibody (A5441 Sigma-Aldrich, St. Louis, MO). Anti-rabbit IgG (A3687 Sigma-Aldrich, St. Louis, USA) and anti-mouse IgG (A1418 Sigma-Aldrich, St. Louis, USA) antibodies conjugated with alkaline phosphatase were used as secondary antibodies.

SUPPLEMENTARY REFERENCES

1 Sandoval J, Heyn H, Moran S et al. Validation of a DNA methylation microarray for 450,000 CpG sites in the human genome. Epigenetics 2011; 6(6): 692–702.

2 Kulis M, Merkel A, Heath S et al. Whole-genome fingerprint of the DNA methylome during human B cell differentiation. Nat Genet 2015; 47(7): 746–756.

3 Agirre X, Castellano G, Pascual M et al. Whole-epigenome analysis in multiple myeloma reveals DNA hypermethylation of B cell-specific enhancers. Genome Res 2015; 25(4): 478–487.

4 Ernst J, Kheradpour P, Mikkelsen TS et al. Mapping and analysis of chromatin state dynamics in nine human cell types. Nature 2011; 473(7345): 43–49.

5 Wijetunga NA, Delahaye F, Zhao YM et al. The meta-epigenomic structure of purified human stem cell populations is defined at cis-regulatory sequences. Nat

Commun 2014; 5: 5195.

6 Mi H, Huang X, Muruganujan A et al. PANTHER version 11: expanded annotation data from Gene Ontology and Reactome pathways, and data analysis tool enhancements. Nucleic Acids Res 2017; 45(D1): D183–D189.

7 Skov V, Larsen TS, Thomassen M et al. Whole-blood transcriptional profiling of interferon-inducible genes identifies highly upregulated IFI27 in primary myelofibrosis. Eur J Haematol 2011; 87(1): 54–60.

8 Ritchie ME, Phipson B, Wu D et al. limma powers differential expression analyses for RNA-sequencing and microarray studies. Nucleic Acids Res 2015; 43(7): e47.

9 Klug M, Rehli M. Functional analysis of promoter CpG methylation using a CpG-free luciferase reporter vector. Epigenetics 2006; 1(3): 127–130.

10 Hotta A, Cheung AYL, Farra N et al. Isolation of human iPS cells using EOS lentiviral vectors to select for pluripotency. Nat Methods 2009; 6(5): 370–376.

SUPPLEMENTARY FIGURE LEGEND

FIGURE S1. *ZFP36L1* is hypermethylated in MF A. Unsupervised dendrogram of DMC between MF and control samples show a distinctive pattern of DNA methylation of MF samples and controls (and no differences between primary and secondary MF). **B)** Schematic representation of *ZFP36L1* locus and the comparative DNA methylation of all CpG dinucleotides included in the array for MF samples (upper panel) and controls samples (lower panel). Vertical bars represent normalized DNA methylation value as per the scale on the left. Chromatin state annotation is depicted on the color-coded horizontal bar on the top. Green boxes represent predicted CpG islands from UCSC genome browser. RefSeq transcript variants are shown in the bottom. **C)** Bisulfite sequencing of the enhancer and promoter region of *ZFP36L1* in peripheral blood cells, different myeloid cell lines and MF patients. Black dots represent methylated and white dots are unmethylated CpG dinucleotides.

SUPPLEMENTARY TABLES

Supplementary Table 1. Lits of primers used for pyrosequencing, gene expression (qPCR) and pCPGL vector cloning.

Supplementary Table 2. Differentially methylated CpG mapped to enhancer regions (FDR<0.05) and expression value of most adjacent gene.

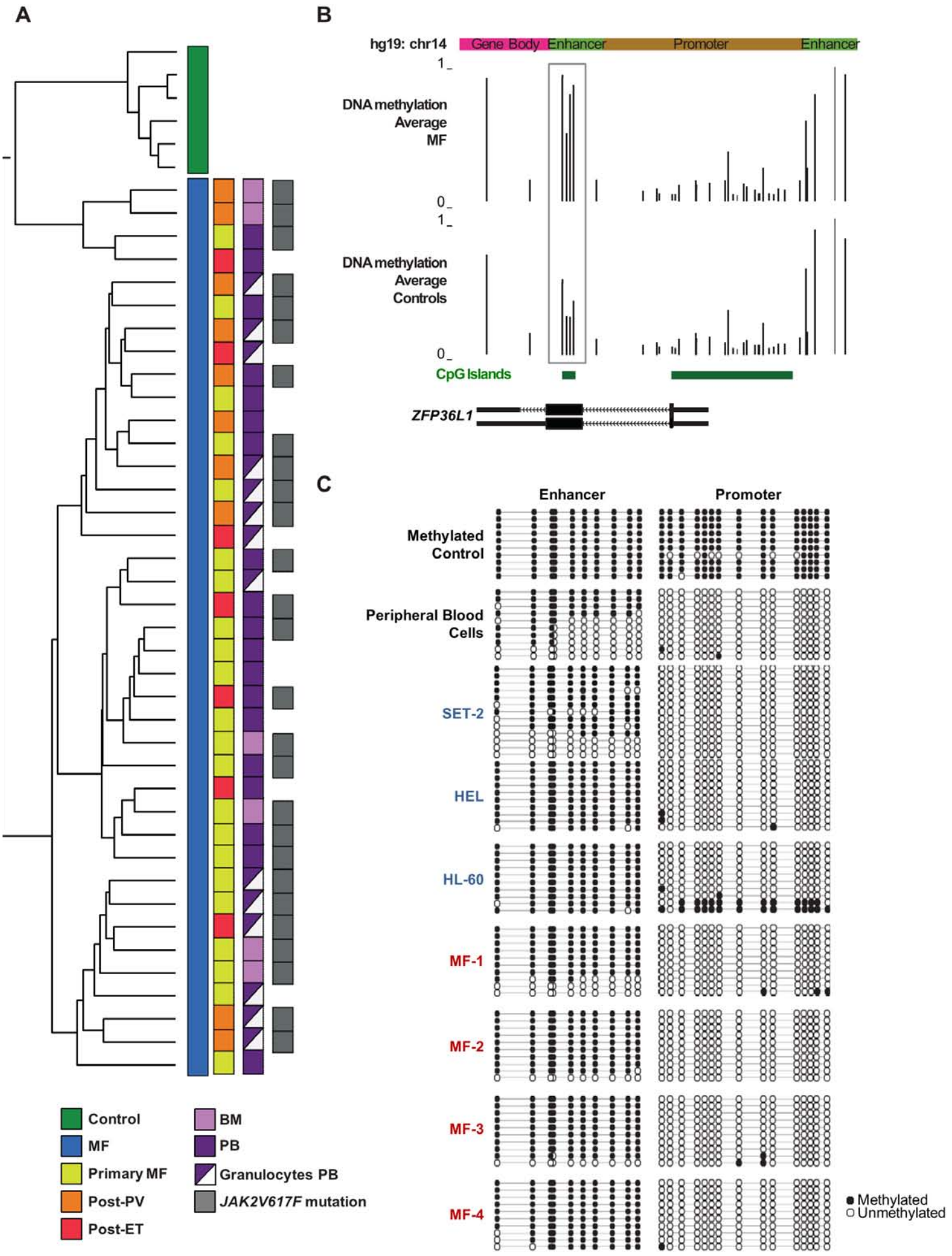

Supplementary Figure 1

Supplementary Table 1. Lits of primers used for pyrosequencing, gene expression (qPCR) and pCPGL vector cloning.

Primers for pyrosequencing and bisulfite sequencing				
Gene	**Primer**	**5´to 3´sequence**	**Size (bp)**	**T°**
ZFP36L1 promoter	*ZFP-PR-F*	gtgacgtactagcaacgGGTTGGAGGGTAGTAGTAGAATAAG	333	**56°C**
	ZFP-PR-R	tagcaggatacgactatcAATTAAATCACCCCATTATAAACAC		
	SP6	TATTTAGGTGACACTATAG	Sequencing primer	
ZFP36L1 enhancer	*ZFP-EH-F*	gtgacgtactagcaacgGTTGTTTTTGGGTGGGTAGTAGT	188	**57°C**
	ZFP-EH-R	tagcaggatacgactatcCACCCCTACTAATAAAAACTTCCCT		
	SP6	TATTTAGGTGACACTATAG	Sequencing primer	

Primers for RT-QPCR experiments				
Gene	**Primer**	**5´to 3´sequence**	**Size (bp)**	**T°**
GUSB	*GUS-RT-Fw*	GAAAATATGTGGTTGGAGAGCTCATT	101	60°C
	GUS-RT-Rv	CCGAGTGAAGATCCCCTTTTTA		
ZFP36L1	*ZFP36L1-RT-Fw*	GATGACCACCACCCTCGT	90	60°C
	ZFP36L1-RT-Rv	CTGGGAGCACTATAGTTGAGCA		

Primers for pCPGL vector experiments				
Gene	**Primer**	**5´to 3´sequence**	**Size (bp)**	**T°**
ZFP36L1 enhancer	*ZFP-EH-F-BamHI*	GTTGTTGGATCCAGCTCCAAGTTCCACCAGAA	534	50°C
	ZFP-EH-F-HindIII	GGTGGTAAGCTTGTCATCGGCGCTCAGAATAG		
Minimal Promoter	*MinProm-F*	CTAGAGAGGGTATATAATGGAAGCTTAACTTCCAG	-	-
	MinProm-R	CTAGCTGGAAGTTAAGCTTCCATTATATACCCTCT	-	-
pCPGL sequencing	*pCPGL-F*	TAAATCTCTTTGTTCAGCTCTCTG	-	-
	pCPGL-R	TTTTCACTGCATTCTAGTTGTGG	-	-
	pCPGL-Fw-short	GTGAGCAAACAGCAGATTAAAAGGA	-	-
	pCPGL-RV-short	GGGACCAGGGCATACCTCTT	-	-